Photosynth Res (2007) 92:357–368
DOI 10.1007/s11120-007-9194-9

MINI REVIEW

# EPR spectroscopy of the manganese cluster of photosystem II

**Alice Haddy**

Received: 7 August 2006 / Accepted: 3 May 2007 / Published online: 6 June 2007


**Abstract** Electron paramagnetic resonance (EPR) spectroscopy is a valuable tool for understanding the oxidation state and chemical environment of the $Mn_4Ca$ cluster of photosystem II. Since the discovery of the multiline signal from the $S_2$ state, EPR spectroscopy has continued to reveal details about the catalytic center of oxygen evolution. At present EPR signals from nearly all of the S-states of the $Mn_4Ca$ cluster, as well as from modified and intermediate states, have been observed. This review article describes the various EPR signals obtained from the $Mn_4Ca$ cluster, including the metalloradical signals due to interaction of the cluster with a nearby organic radical.

**Keywords** Electron paramagnetic resonance · Manganese cluster · Multiline signal · Oxygen evolving complex · Photosystem II · S-state

**Abbreviations**

| | |
|---|---|
| CW-EPR | Continuous wave EPR |
| ENDOR | Electron-nuclear double resonance |
| EPR | Electron paramagnetic resonance |
| ESEEM | Electron spin echo envelop modulation |
| ESE-ENDOR | Electron spin echo ENDOR |
| IR | Infra-red |
| OEC | Oxygen evolving complex |
| PSII | Photosystem II |
| ZFS | Zero field splitting |

A. Haddy (✉)
Department of Chemistry and Biochemistry, University of North Carolina at Greensboro, Greensboro, NC 27402, USA
e-mail: aehaddy@uncg.edu

## Introduction

Since its early applications to biological systems in the 1950s, electron paramagnetic resonance (EPR) spectroscopy has been a valuable tool in understanding the chemistry of metal centers and organic radicals within proteins. It is an ideal technique for studying electron transfer systems such as those found in photosynthetic membranes because it involves the detection of unpaired electrons. As a result, a large body of the photosynthesis literature includes the routine application of EPR spectroscopy. This review focuses on the application of EPR spectroscopy to the manganese cluster ($Mn_4Ca$) of photosystem II (PSII) and the numerous signals obtained from its various oxidation states.

EPR spectroscopy (also known as electron spin resonance or ESR spectroscopy) depends on the absorption of microwave radiation during electron spin-state transitions of one or more unpaired electrons ($S \geq ½$). (For a general explanation of EPR spectroscopy, possible sources include Palmer (1985), Pilbrow (1990), Weil et al. (1994), and Brudvig (1995).) The spin state of the $Mn_4Ca$ cluster is defined by the *coupling of electron spins* of the four Mn ions, which are thought to be dominated primarily by $Mn^{3+}$ and $Mn^{4+}$ during the various S-states. As the $Mn_4Ca$ cluster proceeds through its catalytic cycle, the overall oxidation state of the cluster increases and the mode of coupling between Mn spins is likely to change, with the possibility of more than one coupling scheme in any one S-state. States with spin $S > ½$ may show *zero field splitting* (ZFS), i.e., separation of the $M_S$ energy levels in the absence of a magnetic field, which can lead to observed *g*-factors that are quite different from the ''free electron'' value of 2.0023 and that depend on the operating microwave frequency. EPR absorption lines may be split into multiple

lines by *hyperfine coupling* of the electron spin with one or more nuclear spins, which in the case of a single $^{55}Mn$ nucleus with I = 5/2 can lead to splitting into six lines. Both the *g*-factor and hyperfine coupling constants can show *anisotropy* that arises from inequivalence of principal axes about the spin center, indicating the type of symmetry of the molecular environment. These many possible features combined with the variety of spin states of the $Mn_4Ca$ cluster make it one of the most challenging problems in EPR spectroscopy found in the natural world.

At this point, researchers have obtained EPR signals from nearly all of the S-states of the $Mn_4Ca$ cluster, as well as from modified and intermediate states (Table 1). PSII prepared from higher plants, usually spinach, has been the standard for the study of EPR signals from the $Mn_4Ca$ cluster and this will be the source referred to below unless otherwise indicated. This review will describe those signals obtained from continuous wave (CW) EPR spectroscopy, in which the magnetic field is swept at a constant microwave frequency, usually X-band (9–10 GHz). Although spectra obtained by CW-EPR are influenced by ligands of the metal spin center, the ligand couplings are often not resolved. Interpretation of unresolved ligand couplings has relied on pulsed EPR methods such as electron spin echo envelop modulation (ESEEM) and electron-nuclear double resonance (ENDOR) (Britt et al. 2000). Previous reviews of the application of EPR spectroscopy in the study of the $Mn_4Ca$ cluster include one on the use of pulsed and parallel polarization EPR methods (Britt et al. 2000), an interpretation of results from CW-EPR, pulsed EPR, and X-ray absorption techniques (Åhrling et al. 2005), and a thorough survey of EPR signals from PSII discovered before 1991,

**Table 1** Summary of EPR signals from the manganese cluster of PSII observed at X-band (9–10 GHz)[a]

| S-state and signal[b] | *g*-factor and spin state | Signal features | Sample conditions[c] |
|---|---|---|---|
| $S_2$, MLS | $g = 1.98$, S = ½ | ≥19 lines, 80–90 G spacing | Active, ±alcohols, $Cl^-$ dependent, 140–200 K illum |
| *$S_2$, $Ca^{2+}$-depleted dark-stable MLS* | $g = 2.0$, S = ½ | ≥25 lines, ~55 G spacing | $Ca^{2+}$-depleted, dark adapted up to hours after illum |
| *$S_2$, $NH_3$-modified MLS* | $g = 2.0$, S = ½ | ≥18 lines, 65–70 G spacing | $NH_3$-inhibited, warmed after illum |
| *$S_2$, $Sr^{2+}$-modified MLS* | $g = 2.0$, S = ½ | ≥18 lines, 70–75 G spacing | Replacement of $Ca^{2+}$ with $Sr^{2+}$ |
| $S_2$, $g = 4.1$ signal | $g = 4.1$, S = 5/2 | 340–360 G wide (narrower for inhibited samples) | Active, or anion- or $NH_3$-inhibited, 140–200 K illum or 140–150 K NIR illum of $S_2$ MLS state |
| *$S_2$, $NH_3$-modified $g = 4.1$ signal* | $g = 4.1$, S = 5/2 | ~16 lines, 36 G spacing | $NH_3$-inhibited, oriented, warmed after illum |
| $S_2$, low field signals | $g = 6$, $g = 10$, S ≥ 5/2 | Broad featureless | Active, ~65 K NIR illum of $S_2$ MLS state |
| $S_0$, MLS | $g = 2.0$, S = ½ | 24–26 lines, 80–90 G spacing | Active, flash illuminated (or $NH_2OH$ reduced for $S_0$*), methanol required for hyperfine resolution |
| $S_1$, low field MLS | $g = 12$, (parallel mode), S = 1 | ≥18 lines, 32 G spacing | Lacking PsbP/PsbQ or cyanobacterial |
| $S_1$, $g = 4.8$ signal | $g = 4.8$–$4.9$, (parallel mode), S = 1 | 600 G wide | Active |
| $S_3$ | $g = 8$, $g = 12$, (parallel mode), S = 1 | 300 G, 200 G wide | Active, 235 K illum or flash illum |
| $S_2'$, $g = 5$ signal | $g = 4.7$–$4.8$, $g = 2.9$, S = 7/2 | Broad featureless | Active, 50 K NIR illum or 77 K dark incubation of $S_3$ state |
| $S_3'$ | $g = 21$, $g = 3.7$, S = 1 or 2 | Broad featureless | Active, 4 K NIR illum of $S_3$, then 190 K incubation |
| *$S_2Y_Z$· (inhibited)* | $g = 2.0$, S = ½ with S = ½ radical | Symmetrical ''split'' signal, 100–230 G wide | $Ca^{2+}$-depleted or acetate-, $F^-$, or $NH_3$-inhibited, illum ≥ 250 K |
| $S_0Y_Z$· | $g = 2.0$, S = ½ with S = ½ radical | Symmetrical ''split'' signal, 160 G wide | Active, 4–10 K illum of $S_0$ state |
| $S_1Y_Z$· | $g = 2.035$, $g = 2$, S = 1 with S = ½ radical | Asymmetrical | Active, 4–10 K illum of $S_1$ state or 4 K NIR illum of $S_2$ state |
| $S_2Y_Z$· | $g = 2.0$, S = ½ with S = ½ radical | Symmetrical ''split'' signal, 116 G wide | Active, 77–190 K illum of $S_2$ followed by 77 K, then 10 K |

[a] See text for references. MLS = multiline signal, NIR = near-IR

[b] Inhibited states are given in italics

[c] Illumination is of dark-adapted samples in the $S_1$ state unless otherwise stated. ''Active'' refers to active PSII with intact $Mn_4Ca$ clusters

including most of those from the $S_2$ state (Miller and Brudvig 1991).

## $S_2$ state signals

The $S_2$ state EPR signals are by far the best characterized of all signals from the Mn cluster of PSII because they have been known for the longest time (Dismukes and Siderer 1980, 1981; Casey and Sauer 1984; Zimmermann and Rutherford 1984). They include a multiline signal centered at $g = 2$ and a broad signal centered at $g = 4.1$ (Fig. 1, trace 1). The multiline signal shows a hyperfine pattern that is indicative of Mn nuclear couplings, thereby demonstrating the presence of the Mn cluster that had been long suspected of being at the catalytic center of oxygen evolution. Study of the $S_2$ state signals was facilitated by the development of controlled illumination techniques that produced a single electron transfer from the Mn cluster (Brudvig et al. 1983).

The multiline signal shows 19 or more main hyperfine lines spaced by 80–90 G, indicating that it arises from an antiferromagnetically coupled mixed valence manganese cluster. It is now generally agreed that it arises from the S = ½ ground state of the $Mn_4Ca$ cluster probably in the $Mn^{III}Mn^{IV}{}_3$ valence state. The *g*-tensor and hyperfine pattern have been studied extensively (Dismukes and Siderer 1981; de Paula et al. 1987; Hansson et al. 1987; Haddy et al. 1989; Bonvoisin et al. 1992; Åhrling and Pace 1995; Zheng and Dismukes 1996; Hasegawa et al. 1998; Charlot et al. 2005), since their origin is related to the electronic and geometric structure of the $Mn_4Ca$ site. Studies at Q-band frequency (34 GHz) (Hansson et al. 1987; Smith et al. 1993; Haddy et al. 2004) showed that the signal is generally isotropic, with a central *g*-factor of 1.98. A recent W-band (94 GHz) study using a single crystal of PSII from thermophilic cyanobacteria revealed all three principal *g*-factors of 1.988, 1.981, and 1.965 (Matsuoka et al. 2006). A small amount of hyperfine anisotropy visible in the signal is likely to be contributed by $Mn^{III}$, which typically shows Jahn–Teller distortion. The multiple shoulders that are evident on many of the main hyperfine lines at X-band were resolved in a study of the signal at S-band frequency (3.9 GHz) (Haddy et al. 1989), which revealed 40–50 separate hyperfine lines (Fig. 2). Hyperfine constants of the Mn ions contributing to the multiline signal have been accurately determined using $^{55}$Mn-ENDOR (Peloquin et al. 2000; Kulik et al. 2005), revealing significant contribution from all four Mn ions and axial symmetry for each. Study of the pH dependence of the $S_2$ state multiline signal and the S-state transitions leading to and from it have been carried out (Geijer et al. 2000; Bernát et al. 2002),

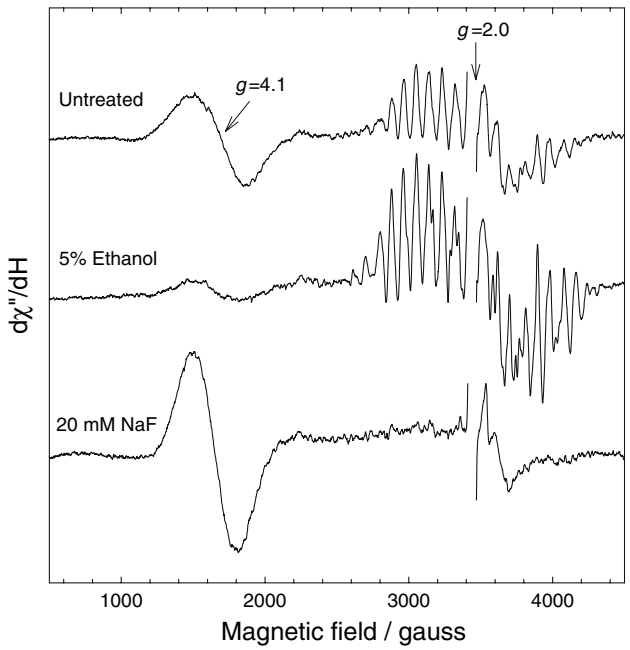


**Fig. 1** Effect of ethanol and fluoride on the $S_2$ state multiline and $g = 4.1$ EPR signals in PSII. PSII-enriched thylakoid membranes from spinach were either untreated, treated with 5% ethanol, or treated with 20 mM NaF, as indicated. For fluoride treatment, the PSII membranes were depleted of chloride by dialysis before NaF addition. Spectra shown are the difference between the states after illumination at 195 K minus the dark-adapted states. Spectra (X-band) were taken at 20 K using 20 mW microwave power

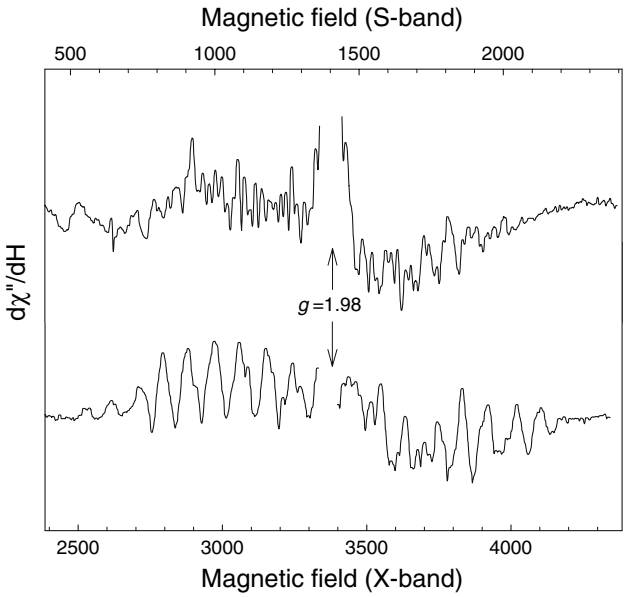


**Fig. 2** S-band (3.9 GHz) and X-band (9.4 GHz) spectra of the $S_2$ state multiline signal. PSII samples were prepared with 2% ethanol and 100 μM DCMU for the S-band spectrum and 4% ethanol for the X-band spectrum. Both spectra are aligned at $g = 1.98$ and cover the same magnetic field width. The S-band spectrum was reproduced from Haddy et al. (1989)

revealing p$K_a$s that are probably associated with the protonation state of side chains ligating the $Mn_4Ca$ cluster.

The signal at $g = 4.1$ has an isotropic appearance with width of 340–360 gauss and no resolved hyperfine structure. This appearance led to an early suggestion that the signal arose from rhombic $Fe^{3+}$ in the S = 5/2 state (Casey and Sauer 1984), but later flash oscillation studies showed that it is associated with the $S_2$ state of the OEC (Zimmermann and Rutherford 1986). Its origin in a Mn cluster was later clarified by the resolution of hyperfine structure with 36 G spacing in samples that were $NH_3$ treated and oriented by partial dehydration (Kim et al. 1990, 1992). The signal arises from the middle Kramers doublet of an S = 5/2 spin state with zero field splitting parameters of $D = 0.455$ cm$^{-1}$ and $E/D = 0.25$. The S = 5/2 spin state was demonstrated by multifrequency EPR studies (Fig. 3) (Haddy et al. 1992, 2004) and supported by pulsed EPR (Astashkin et al. 1994) and SQUID magnetization (Horner et al. 1998) studies. Use of higher-microwave frequencies generally improves the resolution of $g$-factors. At P-band (15 GHz) the signal shows partial resolution of two apparent $g$-factors at 4.7 and 3.85 (Fig. 3, middle spectrum) (Haddy et al. 1992). At Q-band (34 GHz) a broad signal corresponding to only one principal $g$-factor appears at about $g = 3.1$ (Fig. 3, bottom spectrum) (Haddy et al. 2004); the shift in $g$-factor and disappearance of two of the principal axis $g$-factors is indicative of ZFS energy that is comparable to the operating frequency. At X-band the signal shows a $g$-factor of 4.1 rather than 4.3, the position expected for rhombic S = 5/2 systems, because the $Mn_4Ca$ cluster is not completely rhombic, i.e., $E/D = 0.25$ rather than 0.33 which represents complete rhombicity. Another previously observed Q-band signal, with features at about $g = 4.3$ and $g = 4.1$, was identified as the $S_2$ state $g = 4.1$ signal, leading to the suggestion that the signal arose from an S = 3/2 state (Smith et al. 1993; Smith and Pace 1996); however, the identity of this signal has been called into question (Haddy et al. 2004). The X-band $g = 4.1$ signal was thought not to form in cyanobacterial PSII (McDermott et al. 1988; Boussac et al. 1998a), however, it was recently shown that its presence correlates with the cytochrome $c_{550}$ (PsbV) content of the preparation (Lakshmi et al. 2002).

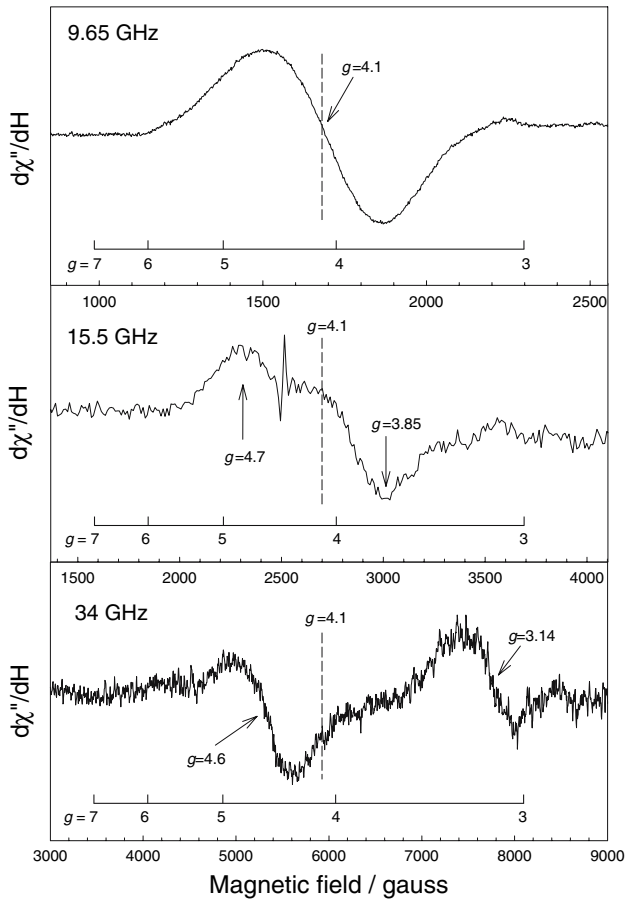


**Fig. 3** Q-band (34 GHz), P-band (15.5 GHz), and X-band (9.65 GHz) spectra of the $S_2$ state $g = 4.1$ signal. The magnetic fields are displayed such that $g$-factor scales are aligned, with spectra centered at $g = 4.1$ (*dashed line*). The Q-band and X-band spectra are reproduced from Haddy et al. (2004). The identity of the Q-band signal at $g = 4.6$ is not clear, but see Haddy et al. (2004) for discussion. The P-band spectrum was previously unpublished, but is similar to those found in Haddy et al. (1992)

Although arising from the same overall valence state, the two $S_2$ state signals show characteristics that indicate they arise from two different spin states of the $Mn_4Ca$ cluster. This is indicated by the influence of the biochemical treatment on their relative intensities, as described in the following paragraphs. It is further supported by temperature-dependence studies of the signal intensities. These experiments, which have proven very difficult to carry out, indicate that both signals are associated with ground spin states (Hansson et al. 1987; Britt et al. 1992; Boussac and Rutherford 2000). The appearance of two different spin states of an exchange-coupled cluster in the same sample (S = ½ and S = 5/2 in this case) is typical of a state of ''spin frustration,'' in which the two spin states have a similar likelihood of occurring.

The two $S_2$ state signals are frequently observed in the same sample, although their relative intensities are affected by the temperature of illumination and the presence of small alcohols, including methanol (3–5%), ethanol (3–5%), and the cryoprotectants glycerol (50%) and ethylene glycol (30%). PSII prepared in the absence of alcohols in sucrose buffer shows both $S_2$ state signals after illumination at 200 K, whereas samples containing small alcohols do not show the $g = 4.1$ signal after illumination at 200 K (Fig. 1, trace 2) (Zimmermann and Rutherford 1986; de Paula et al. 1987; Pace et al. 1991). Samples either with or without small alcohols show the $g = 4.1$ signal but no

multiline signal after illumination at 130–140 K, and upon warming to 200 K intensity is lost from the $g = 4.1$ signal with concurrent formation of the multiline signal (Casey and Sauer 1984; de Paula et al. 1985, 1987). The loss of $g = 4.1$ signal intensity due to the presence of methanol correlates closely with the appearance of multiline signal intensity with an apparent binding constant around 50–65 mM (Force et al. 1998; Deák et al. 1999). Methanol, ethanol, and propanol have been shown to bind at the manganese cluster using ESEEM measurements (Force et al. 1998).

Both $S_2$ state signals are influenced by the presence of $Cl^-$, which is required to fully activate oxygen evolution activity. $Cl^-$ is required for formation of the multiline signal and the signal height has been found to be correlated with oxygen evolution activity (Yachandra et al. 1986). Other activating anions ($Br^-$, $NO_3^-$, $I^-$) have also been found to support multiline signal formation (Damoder et al. 1986; Yachandra et al. 1986; Ono et al. 1987; Lindberg and Andréasson 1996; Olesen and Andréasson 2003; Bryson et al. 2005). On the other hand, $Cl^-$ depletion or substitution of $Cl^-$ with anions such as $F^-$ or $N_3^-$, which are competitors of $Cl^-$ activation, prevent multiline signal formation (Fig. 1, trace 3) (Casey and Sauer 1984; Damoder et al. 1986; Yachandra et al. 1986; Ono et al. 1987; van Vliet and Rutherford 1996; Haddy et al. 2000; Olesen and Andréasson 2003). In one study, the multiline signal was found to form *after* the addition of $Cl^-$ in the dark to $Cl^-$-depleted PSII that had been flash treated (Ono et al. 1986), indicating that oxidizing equivalents to produce the $S_2$ state had been accumulated before the multiline signal had formed. The $g = 4.1$ signal, on the other hand, is able to form whether or not PSII is $Cl^-$ depleted or $Cl^-$ substituted with inhibitory anions such as $F^-$ or $N_3^-$ (Casey and Sauer 1984; Ono et al. 1986, 1987; DeRose et al. 1995; Lindberg and Andréasson 1996; van Vliet and Rutherford 1996; Haddy et al. 2000; Olesen and Andréasson 2003). However, treatment with $F^-$ or $N_3^-$, and possibly $Cl^-$ depletion, results in narrowing of the line width by about 10% (Casey and Sauer 1984; Haddy et al. 1992, 2000), indicating that $Cl^-$ influences the environment of the $g = 4.1$ signal spin center. Several studies have reported enhancement of the $g = 4.1$ signal by $F^-$, which is partially explained by the narrower line width. An approximate inverse correlation was shown between the heights of the $g = 4.1$ signal and the multiline signal in response to $F^-$ concentration (DeRose et al. 1995).

A signal that is virtually identical to the $g = 4.1$ signal is produced by near IR illumination of samples in the $S_2$ state at 140–150 K with concurrent loss of the multiline signal (Boussac et al. 1996, 1998b). The absorbance maximum of this transition is at 820 nm or 12,200 $cm^{-1}$. The formation of the signal under these conditions is thought to be due either to a charge transfer within the $Mn_4Ca$ cluster from $Mn^{III}$ to $Mn^{IV}$ or to a spin-state conversion of $Mn^{III}$. An alternative proposal attributes the near IR absorption to a spin-allowed d-d transition in a single $Mn^{III}$ ion (Baxter et al. 1999). Since the $g = 4.1$ signal formed by near IR illumination relaxes back to the multiline signal at 200 K, the near IR component of broad light sources is not thought to be responsible for the $g = 4.1$ signal observed after illumination at 200 K. The near IR-induced conversion from multiline signal to $g = 4.1$ signal takes place via an intermediate $S \geq 5/2$ spin state characterized by EPR signals at $g = 6$ and $g = 10$, which can be trapped by illumination at about 65 K (Boussac et al. 1998b). Similar intermediate signals at $g = 5$–$9$ have been observed in cyanobacteria (Boussac et al. 1998a), although the near IR-induced $g = 4.1$ signal has not.

A number of treatments produce modified versions of the $S_2$ state multiline signal, most of which have been subsequently found to arise from centers in which the direct ligation to Mn has been altered. PSII treated with the inhibitor ammonia at pH 7.5 shows a multiline signal with line spacings of 65–70 G when binding takes place in the $S_2$ state (Fig. 4, trace 4) (Beck and Brudvig 1986a, b; Andréasson et al. 1988; Ono and Inoue 1988; Boussac et al. 1990a). $NH_3$ binds to two sites at the OEC, one of which is associated with $Cl^-$ activation. Binding of $NH_3$ to the $Cl^-$ activation site causes narrowing of the $g = 4.1$ signal by about 10%, while binding to the non-$Cl^-$ site, which is possibly a water substrate site, modifies the multiline signal. $NH_3$ bound at the latter site has been shown by ESEEM measurements to be directly ligated to the $Mn_4Ca$ cluster (Britt et al. 1989). Substitution of $Sr^{2+}$ for $Ca^{2+}$ at the Mn cluster results in a modified multiline signal with line spacing of 70–75 G (Fig. 4, trace 2) (Boussac and Rutherford 1988; Boussac et al. 1989; Ono and Inoue 1989; Tso et al. 1991; Latimer et al. 1995), similar to the effect of $NH_3$. $Sr^{2+}$ also causes an increase in the intensity of the $g = 4.1$ signal. $Ca^{2+}$ depletion by several methods leads to a ''dark stable'' multiline signal with 25 or more lines of about 55 G spacing (Fig. 4, trace 3) (Boussac et al. 1989; Sivaraja et al. 1989; Ono and Inoue 1990). This signal persists at 0–20°C for up to hours in the dark after illumination, showing that the absence of $Ca^{2+}$ from the Mn cluster stabilizes the $S_2$ state. This signal has been closely associated with the split signal from the inhibited $S_2Y_Z^{\cdot}$ state (see below), which forms after illumination of the same samples.

## $S_0$ state signal

The $S_0$ state shows a multiline signal with 24–26 hyperfine lines with spacings of 80–90 G (Fig. 5) (Åhrling et al.

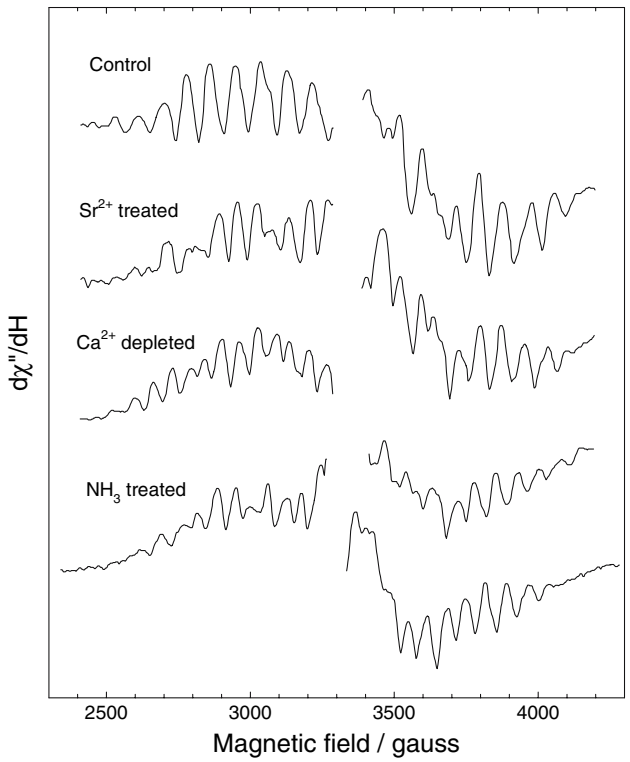


**Fig. 4** Effect of $Ca^{2+}$ depletion, $Sr^{2+}$ treatment, and $NH_3$ treatment on the $S_2$ state multiline signal. For the control, $Ca^{2+}$-depleted, and $Sr^{2+}$-treated PSII samples, $Ca^{2+}$ depletion was carried out using low-pH/citrate treatment, with 50 mM $CaCl_2$ (control) or $SrCl_2$ added as indicated; spectra are reproduced from Latimer et al. (1995). For the $NH_3$-treated sample, the sample was prepared with 50 mM $(NH_4)_2SO_4$ at pH 7.5 and illuminated at 273 K for 30 s to ensure binding of $NH_3$ in the $S_2$ state; the spectrum was reproduced from Andréasson et al. (1988)

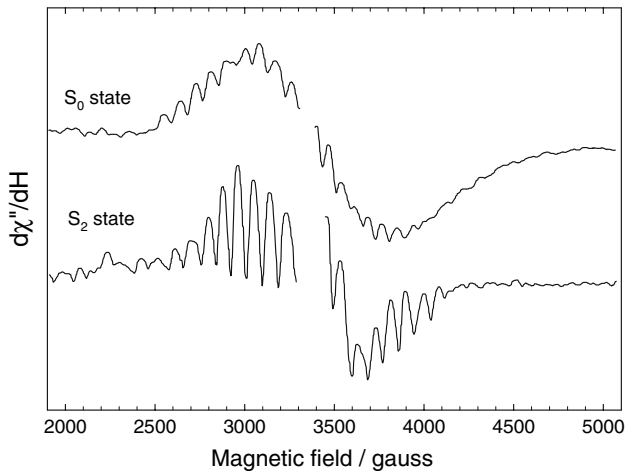


**Fig. 5** $S_0$ state multiline signal compare with the $S_2$ state multiline signal in PSII samples containing 1.5% methanol. The $S_0$ state was prepared by flash advancement of the PSII sample, while the $S_2$ state was produced by continuous illumination at 200 K. Both show difference spectra of the $S_0$ or $S_2$ state minus the $S_1$ state. Spectra were reproduced from Messinger et al. (1997b)

1997; Messinger et al. 1997a, b). The signal is produced by flashing forward through three S-states (Åhrling et al. 1997; Messinger et al. 1997b) or by chemical reduction with hydroxylamine to form the $S_0$* state (Messinger et al. 1997a). The signal originates from an S = ½ ground state (Åhrling et al. 1998), which probably results from coupling within a $Mn^{III}{}_3Mn^{IV}$ or a $Mn^{II}Mn^{III}Mn^{IV}{}_2$ cluster. The hyperfine coupling of the $S_0$ multiline signal is observed only in the presence of methanol, although the broadened signal is observed in its absence. This is reminiscent of the effect of alcohols on improving the resolution of the hyperfine lines of the $S_2$ state multiline signal. $^{55}$Mn-ENDOR has been used to determine the hyperfine constants of the Mn ions contributing to the $S_0$ multiline signal (Kulik et al. 2005), favoring a $Mn^{III}{}_3Mn^{IV}$ assignment of the oxidation state. The pH dependence of the $S_0$ state multiline signal, as well as its formation and loss, has been studied along with the $S_2$ state multiline signal (Geijer et al. 2000; Bernát et al. 2002).

## $S_1$ state signals

Two EPR signals have been detected from the $S_1$ state using parallel mode detection, in which the magnetic field component associated with the microwave radiation is polarized parallel to the applied magnetic field. Parallel mode EPR, as opposed to perpendicular mode used in conventional CW-EPR, is very useful for detecting partially allowed ''$\Delta M_S = 0$'' transitions in integer spin systems. The $S_1$ state, with one more electron than the $S_2$ state, is diamagnetic (S = 0) in the ground state (Koulougliotis et al. 1992), but integer spin excited states of the same spin manifold (S = 1, S = 2, etc.) are accessible.

The first report of an $S_1$ state signal was of a featureless signal at $g$ = 4.8–4.9 with width of about 600 G (Fig. 6a) (Dexheimer and Klein 1992; Yamauchi et al. 1997). This signal is thought to arise from an S = 1 state with ZFS parameters of $D$ = –0.125 to –0.14 $cm^{-1}$ and $E/D$ = –0.20 to –0.25. The S = 1 state is separated from the ground state by about 2.5 K, implying an exchange coupling of $J$ = –0.87 $cm^{-1}$ for a two-spin system (Yamauchi et al. 1997). Methanol and ethylene glycol suppress the signal, as do $Ca^{2+}$ or $Cl^-$ depletion (Yamauchi et al. 1997). The loss of the $S_1$ state $g$ = 4.8 signal upon proceeding to the $S_2$ state appears to correlate with the formation of the $S_2$ state multiline signal, but not with formation of the $g$ = 4.1 signal (Dexheimer and Klein 1992; Yamauchi et al. 1997).

Another $S_1$ state EPR signal appears at about $g$ = 12 and shows 18 or more hyperfine lines with an average splitting of 32 G (Fig. 6b) (Campbell et al. 1998a, b), features characteristic of a Mn cluster. The signal is detected only in higher plant PSII lacking the extrinsic PsbQ and PsbP su-

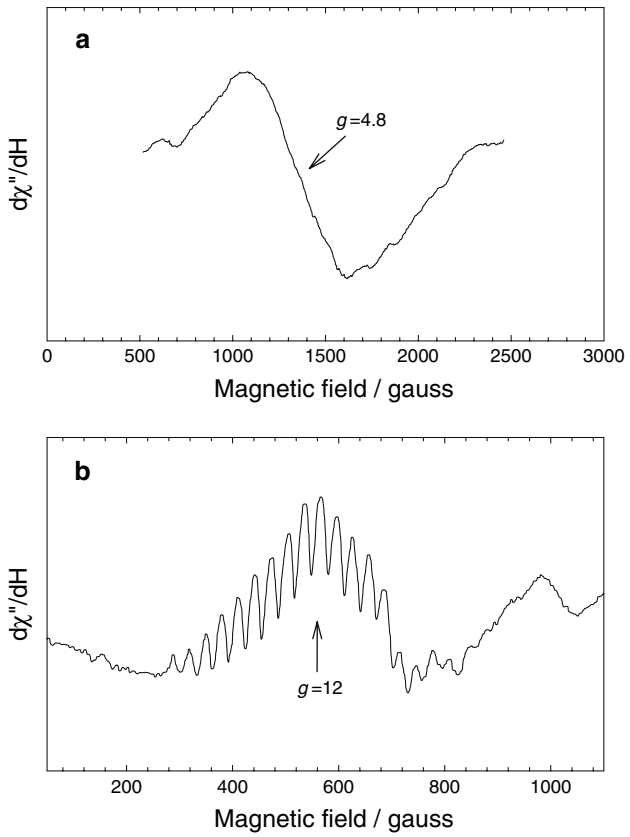


**Fig. 6** $S_1$ state signals, observed using parallel mode detection: (**a**) Signal at $g = 4.8$ in spinach PSII; (**b**) Multiline signal at $g = 12$ in PSII from *Synecocystis* sp. 6803. Both show difference spectra of the $S_1$ state minus the $S_2$ state. Spectrum (**a**) was reproduced from Dexheimer and Klein (1992) and spectrum (**b**) was reproduced from Campbell et al. (1998b)

bunits (17 and 23 kDa) (Campbell et al. 1998a) or in cyanobacterial PSII (Campbell et al. 1998b), which contains PsbU and PsbV (cytochrome $c_{550}$) as dissociable extrinsic subunits. The importance of the extrinsic subunits in observing the $S_1$ state multiline signal indicates that they influence the magnetic properties of the Mn cluster.

## $S_3$ state signals

The $S_3$ state (generated by two flashes of light or by illumination at 235 K) shows EPR signals using parallel and perpendicular mode EPR spectroscopy (Matsukawa et al. 1999; Ioannidis and Petrouleas 2000, 2002; Ioannidis et al. 2002). Parallel mode EPR reveals broad signals at $g = 8$ and $g = 12$ (or $g = 17$ using peak location) with widths of about 300 G and 200 G, respectively. Conventional perpendicular mode reveals a broad signal at $g = 6.7$ (or $g = 10$ using peak location). These signals are thought to arise from an $S = 1$ spin state with ZFS parameters $D = \pm 0.435$ cm$^{-1}$ and $E/D = -0.317$ (Matsukawa et al. 1999). Very similar signals have also been observed in cyanobacterial PSII (Boussac et al. 2000).

## $S_2'$ state and $S_3'$ state signals

Several signals have been observed from states of the $Mn_4Ca$ cluster that are evidently high-spin intermediates of the S-states (reviewed in Petrouleas et al. 2005). A signal is observed at about $g = 5$ ($g = 4.7$–$4.8$) in samples that are prepared in the $S_3$ state and subsequently incubated in liquid $N_2$ for several days (Fig. 7) or illuminated with near IR radiation at 50 K (Nugent et al. 1997; Ioannidis and Petrouleas 2000, 2002; Sanakis et al. 2001). The signal evidently arises from a modified $S_2$ state, referred to as $S_2'$, which is achieved by decay of the $S_3$ state. The $S_2'$ signal at $g = 5$ is thought to arise from an $S = 7/2$ spin state of the $Mn_4Ca$ cluster (Sanakis et al. 2001). The $S_2'$ state also shows a second signal at $g = 2.9$ (Ioannidis et al. 2002), which arises from a different transition of the same spin manifold as the signal at $g = 5$. The signal at $g = 5$ also appears in samples at pH 8.1 after illumination of the $S_1$ state at 243 K (Ioannidis and Petrouleas 2002), suggesting that the signal is associated with a proton-deficient form of the $S_2$ state.

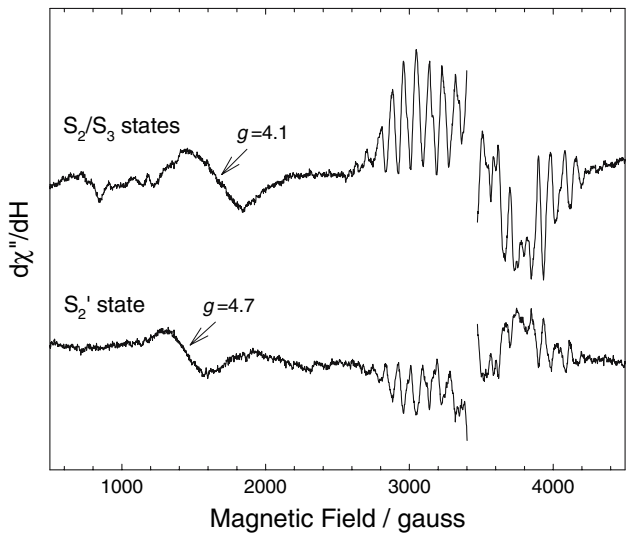


**Fig. 7** Appearance of the $S_2'$ signal at $g = 4.7$ after decay of the $S_3$ state. PSII that had been treated with 0.2 mM atrazine and 2 mM ferricyanide was illuminated at 243 K to induce a mixture of the $S_2$ and $S_3$ states (*top*), then incubated at 77 K for 11 days resulting in decay of the $S_3$ state to the $S_2'$ state (*bottom*). The top difference spectrum shows the state after 243 K illumination ($S_2/S_3$) minus the dark-adapted state ($S_1$). The bottom difference spectrum shows the state after 77 K incubation ($S_2'$) minus the top spectrum; the negative multiline signal shows decay of the $S_2$ state. Spectra were taken at 10 K using 20 mW microwave power

Additional EPR signals have been observed in samples prepared in the $S_3$ state, illuminated with near IR radiation at 4 K, then warmed to 190 K, leading to a modified $S_3$ state ($S_3'$). These appear at $g = 21$ and $g = 3.7$ using perpendicular mode EPR spectroscopy (Ioannidis et al. 2002) and arise from an integer spin state of the $Mn_4Ca$ cluster.

## Metalloradical signals

Several signals from the OEC appearing at $g = 2$ are attributed to the interaction between an organic free radical, usually identified as Tyr Z, and the $Mn_4Ca$ cluster (for a summary see Petrouleas et al. 2005). The first metalloradical signal of this type to be observed was a symmetrical 130–165 G wide ''split'' signal from $Ca^{2+}$-depleted PSII (Boussac et al. 1989, 1990b; Sivaraja et al. 1989; Ono and Inoue 1990; Hallahan et al. 1992), which appears to consist of two lines (Fig. 8, trace 4). It is produced by illumination of samples showing the ''dark stable'' $S_2$ state multiline signal (described above) at or above 250 K. The signal shows fast relaxation properties typical of a spin S = ½ radical interacting with a paramagnet, which in this case is the S = ½ spin state of the modified $S_2$ state Mn cluster. Similar signals, with line widths depending on the treatment, are produced in PSII samples containing high concentrations of acetate (230 G wide) (MacLachlan and Nugent 1993; Szalai and Brudvig 1996), fluoride (160 G wide) (Baumgarten et al. 1990), or $NH_3$ (100 G wide) (Andréasson and Lindberg 1992; Hallahan et al. 1992). In addition, a very similar signal that is 90–100 G wide has been produced in active PSII samples in the $S_3$ state by elevation of the pH above 8.5 (Geijer et al. 2001). ESE-ENDOR and ESEEM studies of $Ca^{2+}$-depleted and acetate-treated PSII have identified the radical as Tyr Z (Gilchrist et al. 1995; Peloquin et al. 1998), although a His radical has also been proposed (Boussac et al. 1990b). The signal has therefore been assigned to the $S_2Y_Z\cdot$ state. Extensive study using multifrequency EPR spectroscopy has revealed details about the dipolar couplings and exchange interactions in the $Ca^{2+}$-depleted and acetate-treated $S_2Y_Z\cdot$ states (Lakshmi et al. 1998; Dorlet et al. 1999). The $Ca^{2+}$-depleted system has under some conditions been suggested to include two signals in the $g = 2$ region, a symmetric doublet signal and an asymmetric singlet-like signal (Astashkin et al. 1997; Mino et al. 2000).

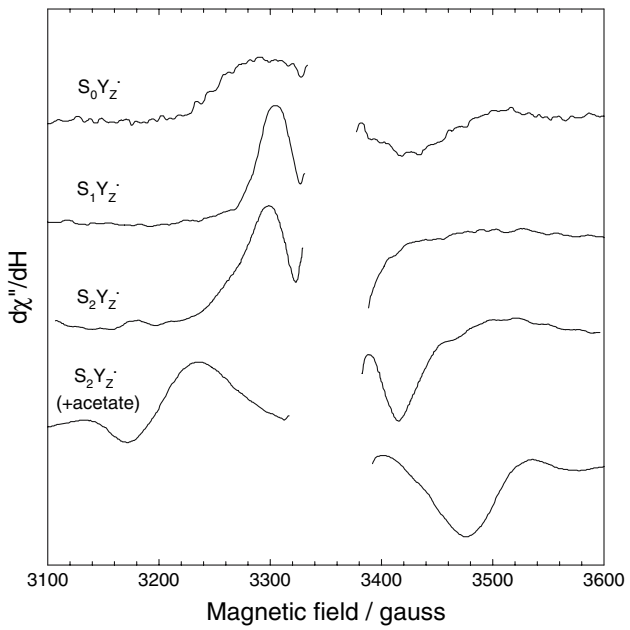


**Fig. 8** Metalloradical signals from the $S_0Y_{\dot{Z}}$ state, $S_1Y_Z$ state, $S_2Y_Z$ state, and inhibited $S_2Y_{\dot{Z}}$ (+acetate) state. The $S_0Y_Z$ and $S_1Y_{\dot{Z}}$ signals correspond to the states produced by 4–10 K illumination of PSII in the $S_0$ and $S_1$ states, respectively. The $S_2Y_{\dot{Z}}$ signal corresponds to the state produced after flash illumination of the $S_2$ state at 190 K, followed by rapid cooling to 77 K, then 10 K. The $S_2Y_{\dot{Z}}$ (+acetate) signal corresponds to the state produced by room temperature illumination of PSII in the presence of ~500 mM acetate. The $S_0Y_{\dot{Z}}$, $S_1Y_{\dot{Z}}$, and $S_2Y_{\dot{Z}}$ (+acetate) spectra are reproduced from Petrouleas et al. (2005); the $S_2Y_{\dot{Z}}$ spectrum is reproduced from Ioannidis et al. (2006)

Since $Mn_4Ca$ donates an electron to the reaction center via $Y_Z$, one would expect the presence of an intermediate involving the $Y_Z$ radical on each S-state transition. Indeed, metalloradical signals have been observed for several S-states in uninhibited PSII with intact, $Ca^{2+}$-containing $Mn_4Ca$ clusters. These signals decay within minutes even at liquid helium temperatures. Observation of those associated with the two lower S-states relies on illumination below 10 K to prevent oxidation of the $Mn_4Ca$ cluster. A signal attributed to the $S_1Y_Z\cdot$ state has been observed after illumination of PSII samples in the $S_1$ state or after near IR illumination of samples in the $S_2$ state (Fig. 8, trace 2) (Nugent et al. 2002; Koulougliotis et al. 2003; Zhang and Styring 2003). The signal is typified by a peak at $g = 2.035$, but also includes a line at $g = 2.0$. The signal is produced by the interaction of the S = ½ organic radical with the S = 1 excited spin state of the $S_1$ state $Mn_4Ca$ cluster, as demonstrated by simulation of EPR data from both X-band and W-band (94 GHz) (Koulougliotis et al. 2004). Another metalloradical signal attributed to the $S_0Y_Z\cdot$ state has been observed at $g = 2.0$ after 5 K illumination of PSII samples in the $S_0$ state (Fig. 8, trace 1) (Zhang and Styring 2003). This 160-G-wide signal has a symmetrical appearance similar to that of the ''split'' signal from the $Ca^{2+}$-depleted $S_2Y_Z\cdot$ state. Similar to the $S_2Y_Z\cdot$ signal, it is produced by the interaction of an S = ½ organic radical with the S = ½ spin state of the $S_0$ state $Mn_4Ca$ cluster. The $S_0Y_Z\cdot$ and $S_1Y_Z\cdot$ metalloradical signals have also been observed in cyanobacteria (Zhang et al. 2004).

More recently, a signal attributed to the $S_2Y_Z\cdot$ state has been observed in uninhibited PSII (Fig. 8, trace 3) (Ioannidis et al. 2006). This 116 G-wide signal is produced by flash illumination of the $S_2$ state at 77–190 K, followed by rapid cooling to 77 K, then 10 K.

## Summary

Through the use of EPR spectroscopy, nearly all of the S-states and many intermediate states have been characterized. The results support the basic picture of the OEC's catalytic cycle as involving a cluster of four coupled Mn ions that increase in valence state as the S-states advance, with the $S_0$ and $S_2$ states present as half integer spin states and the $S_1$ and $S_3$ states present as integer spin states lying above zero spin ground states. Specific valences and coupling schemes of the S-states are supported by various simulation studies. The recent discovery of several intermediate state signals involving an interaction of the $Y_Z$ radical with the intact $Mn_4Ca$ cluster correlates well with our understanding of $Y_Z$ as the direct electron donor to $Mn_4Ca$. We seem to be on the verge of correlating the parameters of the EPR signals with specific structural features of the OEC that are revealed by the recent X-ray crystallography studies (Zouni et al. 2001; Kamiya and Shen 2003; Biesiadka et al. 2004; Ferreira et al. 2004; Loll et al. 2005), made possible by the increasing resolution of those studies.

At a deeper level, the many signals discovered by the EPR studies indicate a more complicated picture that is so far only partially understood, but provides clues to the details of the catalytic mechanism. The presence of more than one signal in many of the states (e.g., the multiline and $g = 4.1$ signals in the $S_2$ state, the low field multiline and $g = 4.8$ signals in the $S_1$ state) is suggestive of a flexibility of coupling that may be important for a cluster that must move easily from one oxidation state to another. The influence of protonated states (pH), various ions, alcohols, and other affectors on many of the signals reveals points where a ligating amino acid is involved, an ion is required as cofactor, or a substrate $H_2O$ molecule has access to the $Mn_4Ca$ cluster. The recurrent theme of sensitivity to near IR radiation is suggestive of a key bond or point of electron transfer that is common to many of the S-states. These details will take time and much further study to interpret, but are the ones that will eventually lead to a full understanding of how the electron donor $H_2O$ is converted to $O_2$.

**Acknowledgement** I would like to thank Lars-Erik Andréasson, R. David Britt, Johannes Messinger, Vasili Petrouleas, and Kenneth Sauer for permission to reproduce here the excellent examples of classic signals from their earlier work.

## References

Åhrling KA, Pace RJ (1995) Simulation of the $S_2$ state multiline electron paramagnetic resonance signal of photosystem II: a multifrequency approach. Biophys J 68:2081–2090

Åhrling KA, Peterson S, Styring S (1997) An oscillating manganese electron paramagnetic resonance signal from the $S_0$ state of the oxygen evolving complex in photosystem II. Biochemistry 36:13148–13152

Åhrling KA, Peterson S, Styring S (1998) The $S_0$ state EPR signal from the Mn cluster in photosystem II arises from an isolated S = 1/2 ground state. Biochemistry 37:8115–8120

Åhrling KA, Pace RJ, Evans MCW (2005) The catalytic manganese cluster: implications from spectroscopy. In: Wydrzynski T, Satoh K (eds), Photosystem II: the light-driven water:plastoquinone oxidoreductase. Springer, The Netherlands

Andréasson L-E, Lindberg K (1992) The inhibition of photosynthetic oxygen evolution by ammonia probed by EPR. Biochim Biophys Acta 1100:177–183

Andréasson L-E, Hansson Ö, von Schenck K (1988) The interaction of ammonia with the photosynthetic oxygen-evolving system. Biochim Biophys Acta 936:351–360

Astashkin AV, Kodera Y, Kawamori A (1994) Pulsed EPR study of manganese $g = 4.1$ signal in plant photosystem II. J Magn Reson B 105:113–119

Astashkin AV, Mino H, Kawamori A, Ono T-A (1997) Pulsed EPR study of the $S_3'$ signal in the $Ca^{2+}$-depleted photosystem II. Chem Phys Lett 272:506–516

Baumgarten M, Philo JS, Dismukes GC (1990) Mechanism of photoinhibition of photosynthetic water oxidation by $Cl^-$ depletion and $F^-$ substitution: oxidation of a protein residue. Biochemistry 29:10814–10822

Baxter R, Krausz E, Wydrzynski T, Pace RJ (1999) Identification of the near-infrared absorption band from the Mn cluster of photosystem II. J Am Chem Soc 121:9451–9452

Beck WF, Brudvig GW (1986a) Ammonia binds to the manganese site of the $O_2$–evolving complex of photosystem II in the $S_2$ state. J Am Chem Soc 108:4018–4022

Beck WF, Brudvig GW (1986b) Binding of amines to the $O_2$-evolving center of Photosystem II. Biochemistry 25:6479–6486

Bernát G, Morvaridi F, Feyziyev Y, Styring S (2002) pH dependence of the four individual transitions in the catalytic S-cycle during photosynthetic oxygen evolution. Biochemistry 41:5830–5843

Biesiadka J, Loll B, Kern J, Irrgang K-D, Zouni A (2004) Crystal structure of cyanobacterial photosystem II at 3.2 Å resolution: a closer look at the Mn-cluster. Phys Chem Chem Phys 6:4733–4736

Bonvoisin J, Blondin G, Girerd J-J, Zimmermann J-L (1992) Theoretical study of the multiline EPR signal from the $S_2$ state of the oxygen evolving complex of photosystem II. Biophys J 61:1076–1086

Boussac A, Rutherford AW (1988) Nature of the inhibition of the oxygen-evolving enzyme of photosystem II induced by NaCl washing and reversed by the addition of $Ca^{2+}$ and $Sr^{2+}$. Biochemistry 27:3476–3483

Boussac A, Rutherford AW (2000) Comparative study of the $g = 4.1$ EPR signals in the $S_2$ state of photosystem II. Biochim Biophys Acta 1457:145–156

Boussac A, Zimmermann J-L, Rutherford AW (1989) EPR signals from modified charge accumulation states of the oxygen evolving enzyme in $Ca^{2+}$-deficient Photosystem II. Biochemistry 28:8984–8989

Boussac A, Rutherford AW, Styring S (1990a) Interaction of ammonia with the water splitting enzyme of photosystem II. Biochemistry 29:24–32

Boussac A, Zimmermann J-L, Rutherford AW, Lavergne J (1990b) Histidine oxidation in the oxygen-evolving photosystem-II enzyme. Nature 347:303–306

Boussac A, Girerd J-J, Rutherford AW (1996) Conversion of the spin state of the manganese complex in photosystem II induced by near-infrared light. Biochemistry 35:6984–6989

Boussac A, Kuhl H, Un S, Rögner M, Rutherford AW (1998a) Effect of near-infrared light on the $S_2$-state of the manganese complex of photosystem II from *Synechococcus elongatus*. Biochemistry 37:8995–9000

Boussac A, Un S, Horner O, Rutherford AW (1998b) High-spin states ($S \geq 5/2$) of the Photosystem II manganese complex. Biochemistry 37:4001–4007

Boussac A, Sugiura M, Inoue Y, Rutherford AW (2000) EPR study of the oxygen evolving complex in His-tagged photosystem II from the cyanobacterium *Synechococcus elongatus*. Biochemistry 39:13788–13799

Britt RD, Zimmermann J-L, Sauer K, Klein MP (1989) Ammonia binds to the catalytic Mn of the oxygen evolving complex of photosystem II: evidence by electron spin echo envelope modulation spectroscopy. J Am Chem Soc 111:3522–3532

Britt RD, Lorigan GA, Sauer K, Klein MP, Zimmermann J-L (1992) The $g = 2$ multiline EPR signal of the $S_2$ state of the photosynthetic oxygen-evolving complex originates from a ground spin state. Biochim Biophys Acta 1140:95–101

Britt RD, Peloquin JM, Campbell KA (2000) Pulsed and parallel-polarization EPR characterization of the photosystem II oxygen-evolving complex. Annu Rev Biophys Biomol Struct 29:463–495

Brudvig GW (1995) Electron paramagnetic resonance spectroscopy. Methods Enzymol 246:536–554

Brudvig GW, Casey JL, Sauer K (1983) The effect of temperature on the formation and decay of the multiline EPR signal species associated with photosynthetic oxygen evolution. Biochim Biophys Acta 723:366–371

Bryson DI, Doctor N, Johnson R, Baranov S, Haddy A (2005) Characteristics of iodide activation and inhibition of oxygen evolution by photosystem II. Biochemistry 44:7354–7360

Campbell KA, Gregor W, Pham DP, Peloquin JM, Debus RJ, Britt RD (1998a) The 23 and 17 kDa extrinsic proteins of photosystem II modulate the magnetic properties of the $S_1$-state manganese cluster. Biochemistry 37:5039–5045

Campbell KA, Peloquin JM, Pham DP, Debus RJ, Britt RD (1998b) Parallel polarization EPR detection of an $S_1$-state ''multiline'' EPR signal in photosystem II particles from *Synechocystis* sp. PCC 6803. J Am Chem Soc 120:447–448

Casey JL, Sauer K (1984) EPR detection of a cryogenically photogenerated intermediate in photosynthetic oxygen evolution. Biochim Biophys Acta 767:21–28

Charlot M-F, Boussac A, Blondin G (2005) Towards a spin coupling model for the $Mn_4$ cluster in photosystem II. Biochim Biophys Acta 1708:120–132

Damoder R, Klimov VV, Dismukes GC (1986) The effect of $Cl^-$ depletion and $X^-$ reconstitution on the oxygen-evolution rate, the yield of the multiline manganese EPR signal and EPR Signal II in the isolated photosystem-II complex. Biochim Biophys Acta 848:378–391

Deák Z, Peterson S, Geijer P, Åhrling K, Styring S (1999) Methanol modification of the electron paramagnetic signals from the $S_0$ and $S_2$ states of the water-oxidizing complex of photosystem II. Biochim Biophys Acta 1412:240–249

de Paula JC, Innes JB, Brudvig GW (1985) Electron transfer in photosystem II at cryogenic temperatures. Biochemistry 24:8114–8120

de Paula JC, Beck WF, Miller A-F, Wilson RB, Brudvig GW (1987) Studies of the manganese site of photosystem II by electron spin resonance spectroscopy. J Chem Soc Faraday Trans 83:3635–3651

DeRose VJ, Latimer MJ, Zimmermann J-L, Mukerji I, Yachandra VK, Sauer K, Klein MP (1995) Fluoride substitution in the Mn cluster from photosystem II: EPR and X-ray absorption spectroscopy studies. Chem Phys 194:443–459

Dexheimer SL, Klein MP (1992) Detection of a paramagnetic intermediate in the $S_1$ state of the photosynthetic oxygen-evolving complex. J Am Chem Soc 114:2821–2826

Dismukes GC, Siderer Y (1980) EPR spectroscopic observations of a manganese center associated with water oxidation in spinach chloroplasts. FEBS Lett 121:78–80

Dismukes GC, Siderer Y (1981) Intermediates of a polynuclear manganese center involved in photosynthetic oxidation of water. Proc Natl Acad Sci 78:274–278

Dorlet P, Boussac A, Rutherford AW, Un S (1999) Multifrequency high-field EPR study of the interaction between the Tyrosyl Z radical and the manganese cluster in plant photosystem II. J Phys Chem B 103:10945–10954

Ferreira KN, Iverson TM, Maghlaoui K, Barber J, Iwata S (2004) Architecture of the photosynthetic oxygen-evolving center. Science 303:1831–1838

Force DA, Randall DW, Lorigan GA, Clemens KL, Britt RD (1998) ESEEM studies of alcohol binding to the manganese cluster of the oxygen evolving complex of photosystem II. J Am Chem Soc 120:13321–13333

Geijer P, Deák Z, Styring S (2000) Proton equilibria in the manganese cluster of Photosystem II control the intensities of the $S_0$ and $S_2$ state g ~ 2 electron paramagnetic resonance signals. Biochemistry 39:6763–6772

Geijer P, Morvaridi F, Styring S (2001) The $S_3$ state of the oxygen-evolving complex in photosystem II is converted to the $S_2Y_Z^\bullet$ state at alkaline pH. Biochemistry 40:10881–10891

Gilchrist ML Jr, Ball JA, Randall DW, Britt RD (1995) Proximity of the manganese cluster of photosystem II to the redox-active tyrosine $Y_Z$. Proc Natl Acad Sci 92:9545–9549

Haddy A, Aasa R, Andréasson L-E (1989) S-band EPR studies of the $S_2$-state multiline signal from the photosynthetic oxygen-evolving complex. Biochemistry 28:6954–6959

Haddy A, Dunham WR, Sands RH, Aasa R (1992) Multifrequency EPR investigations into the origin of the $S_2$-state signal at $g = 4$ of the $O_2$-evolving complex. Biochim Biophys Acta 1099:25–34

Haddy A, Kimel RA, Thomas R (2000) Effects of azide on the $S_2$ state EPR signals from photosystem II. Photosyn Res 63:35–45

Haddy A, Lakshmi KV, Brudvig GW, Frank HA (2004) Q-band EPR of the $S_2$ state of Photosystem II confirms an $S = 5/2$ origin of the X-band $g = 4.1$ signal. Biophys J 87:2885–2896

Hallahan BJ, Nugent JHA, Warden JT, Evans MCW (1992) Investigation of the origin of the ''S3'' EPR signal from the oxygen-evolving complex of Photosystem 2: the role of Tyrosine Z. Biochemistry 31:4562–4573

Hansson Ö, Aasa R, Vänngård T (1987) The origin of the multiline and $g = 4.1$ electron paramagnetic resonance signals from the oxygen-evolving system of photosystem II. Biophys J 51:825–832

Hasegawa K, Kusunoki M, Inoue Y, Ono T-A (1998) Simulation of $S_2$-state multiline EPR signal in oriented photosystem II membranes: structural implications for the manganese cluster in an oxygen-evolving complex. Biochemistry 37:9457–9465

Horner O, Rivière E, Blondin G, Un S, Rutherford AW, Girerd J-J (1998) SQUID magnetization study of the infrared-induced spin transition in the $S_2$ state of photosystem II: spin value associated with the $g = 4.1$ EPR signal. J Am Chem Soc 120:7924–7928

Ioannidis N, Petrouleas V (2000) Electron paramagnetic resonance signals from the $S_3$ state of the oxygen-evolving complex. A

broadened radical signal induced by low-temperature near-infrared light illumination. Biochemistry 39:5246–5254

Ioannidis N, Petrouleas V (2002) Decay products of the $S_3$ state of the oxygen-evolving complex of Photosystem II at cryogenic temperatures. Pathways to the formation of the S = 7/2 $S_2$ state configuration. Biochemistry 41:9580–9588

Ioannidis N, Nugent JHA, Petrouleas V (2002) Intermediates of the S3 state of the oxygen-evolving complex of photosystem II. Biochemistry 41:9589–9600

Ioannidis N, Zahariou G, Petrouleas V (2006) Trapping of the $S_2$ to $S_3$ state intermediate of the oxygen-evolving complex of photosystem II. Biochemistry 45:6252–6259

Kamiya N, Shen J-R (2003) Crystal structure of oxygen-evolving photosystem II from *Thermosynechococcus vulcanus* at 3.7-Å resolution. Proc Natl Acad Sci 100:98–103

Kim DH, Britt RD, Klein MP, Sauer K (1990) The $g = 4.1$ EPR signal of the $S_2$ state of the photosynthetic oxygen-evolving complex arises from a multinuclear Mn cluster. J Am Chem Soc 112:9389–9391

Kim DH, Britt RD, Klein MP, Sauer K (1992) The manganese site of the photosynthetic oxygen-evolving complex probed by EPR spectroscopy of oriented photosystem II membranes: the $g = 4$ and $g = 2$ multiline signals. Biochemistry 31:541–547

Koulougliotis D, Hirsh DJ, Brudvig GW (1992) The $O_2$-evolving center of photosystem II is diamagnetic in the $S_1$ resting state. J Am Chem Soc 114:8322–8323

Koulougliotis D, Shen J-R, Ioannidis N, Petrouleas V (2003) Near-IR irradiation of the $S_2$ state of the water oxidizing complex of Photosystem II at liquid helium temperatures produces the metalloradical intermediate attributed to $S_1Y_Z$-dot. Biochemistry 42:3045–3053

Koulougliotis D, Teutloff C, Sanakis Y, Lubitz W, Petrouleas V (2004) The $S_1Y_{Z\cdot}$ metalloradical intermediate in photosystem II: an X- and W-band EPR study. Phys Chem Chem Phys 6:4859–4863

Kulik LV, Epel B, Lubitz W, Messinger J (2005) $^{55}$Mn pulse ENDOR at 34 GHz of the $S_0$ and $S_2$ states of the oxygen-evolving complex in photosystem II. J Am Chem Soc 127:2392–2393

Lakshmi KV, Eaton SS, Eaton GR, Frank HA, Brudvig GW (1998) Analysis of dipolar and exchange interactions between manganese and Tyrosine Z in the $S_2Y_Z$-dot state of acetate-inhibited Photosystem II via EPR spectral simulations at X- and Q-bands. J Phys Chem B 102:8327–8335

Lakshmi KV, Reifler MJ, Chisholm DA, Wang JY, Diner BA, Brudvig GW (2002) Correlation of the cytochrome $c_{550}$ content of cyanobacterial Photosystem II with the EPR properties of the oxygen-evolving complex. Photosyn Res 72:175–189

Latimer MJ, DeRose VJ, Mukerji I, Yachandra VK, Sauer K, Klein MP (1995) Evidence for the proximity of calcium to the manganese cluster of photosystem II: determination by X-ray absorption spectroscopy. Biochemistry 34:10898–10909

Lindberg K, Andréasson L-E (1996) A one-site, two-state model for the binding of anions in photosystem II. Biochemistry 35:14259–14267

Loll B, Kern J, Saenger W, Zouni A, Biesiadka J (2005) Towards complete cofactor arrangement in the 3.0 Å resolution structure of photosystem II. Nature 438:1040–1044

MacLachlan DJ, Nugent JHA (1993) Investigation of the S3 electron paramagnetic resonance signal from the oxygen-evolving complex of Photosystem 2: effect of inhibition of oxygen evolution by acetate. Biochemistry 32:9772–9780

Matsukawa T, Mino H, Yoneda D, Kawamori A (1999) Dual-mode EPR study of new signals from the $S_3$-state of oxygen-evolving complex in photosystem II. Biochemistry 38:4072–4077

Matsuoka H, Furukawa K, Kato T, Mino H, Shen J-R, Kawamori A (2006) $g$-anisotropy of the $S_2$-state manganese cluster in single crystals of cyanobacterial photosystem II studied by W-band electron paramagnetic resonance spectroscopy. J Phys Chem B 110:13242–13247

McDermott AE, Yachandra VK, Guiles RD, Cole JL, Dexheimer SL, Britt RD, Sauer K, Klein MP (1988) Characterization of the manganese $O_2$-evolving complex and the iron-quinone acceptor complex in Photosystem II from a thermophilic cyanobacterium by electron paramagnetic resonance and x-ray absorption spectroscopy. Biochemistry 27:4021–4031

Messinger J, Nugent JHA, Evans MCW (1997a) Detection of an EPR multiline signal for the $S_0$* state in photosystem II. Biochemistry 36:11055–11060

Messinger J, Robblee JH, Yu WO, Sauer K, Yachandra VK, Klein MP (1997b) The $S_0$ state of the oxygen-evolving complex in photosystem II is paramagnetic: detection of an EPR multiline signal. J Am Chem Soc 119:11349–11350

Miller A-F, Brudvig GW (1991) A guide to electron paramagnetic resonance spectroscopy of photosystem II membranes. Biochim Biophys Acta 1056:1–18

Mino H, Kawamori A, Ono T-A (2000) Pulsed EPR studies of doublet signal and singlet-like signal in oriented $Ca^{2+}$-depleted PS II membranes: location of the doublet signal center in PS II. Biochemistry 39:11034–11040

Nugent JHA, Turconi S, Evans MCW (1997) EPR investigation of water oxidizing photosystem II: detection of new EPR signals at cryogenic temperatures. Biochemistry 36:7086–7096

Nugent JHA, Muhiuddin IP, Evans MCW (2002) Electron transfer from the water oxidizing complex at cryogenic temperatures: the $S_1$ to $S_2$ step. Biochemistry 41:4117–4126

Olesen K, Andréasson L-E (2003) The function of the chloride ion in photosynthetic oxygen evolution. Biochemistry 42:2025–2035

Ono T-A, Inoue Y (1988) Abnormal S-state turnovers in $NH_3$-binding Mn centers of photosynthetic $O_2$ evolving system. Arch Biochem Biophys 264:82–92

Ono T-A, Inoue Y (1989) Roles of $Ca^{2+}$ in $O_2$ evolution in higher plant photosystem II: effects of replacement of $Ca^{2+}$ site by other anions. Arch Biochem Biophys 275:440–448

Ono T-A, Inoue Y (1990) Abnormal redox reactions in photosynthetic $O_2$-evolving centers in NaCl/EDTA-washed PS II. A dark-stable EPR multiline signal and an unknown positive charge accumulator. Biochim Biophys Acta 1020:269–277

Ono T-A, Zimmermann J-L, Inoue Y, Rutherford AW (1986) EPR evidence for a modified S-state transition in chloride-depleted photosystem II. Biochim Biophys Acta 851:193–201

Ono T-A, Nakayama H, Gleiter H, Inoue Y, Kawamori A (1987) Modification of the properties of $S_2$ state in photosynthetic $O_2$-evolving center by replacement of chloride with other anions. Arch Biochem Biophys 256:618–624

Pace RJ, Smith PJ, Bramley R, Stehlik D (1991) EPR saturation and temperature dependence studies on signals from the oxygen-evolving centre of photosystem II. Biochim Biophys Acta 1058:161–170

Palmer G (1985) The electron paramagnetic resonance of metalloproteins. Biochem Soc Trans 13:548–560

Peloquin JM, Campbell KA, Britt RD (1998) $^{55}$Mn pulsed ENDOR demonstrates that the Photosystem II ''split'' EPR signal arises from a magnetically-coupled mangano-tyrosyl complex. J Am Chem Soc 120:6840–6841

Peloquin JM, Campbell KA, Randall DW, Evanchik MA, Pecoraro VL, Armstrong WH, Britt RD (2000) $^{55}$Mn ENDOR of the $S_2$-state multiline EPR signal of photosystem II: implications on the structure of the tetranuclear Mn cluster. J Am Chem Soc 122:10926–10942

Petrouleas V, Koulougliotis D, Ioannidis N (2005) Trapping of metalloradical intermediates of the S-states at liquid helium

temperatures. Overview of the phenomenology and mechanistic implications. Biochemistry 44:6723–6728

Pilbrow JR (1990) Transition ion electron paramagnetic resonance. Oxford University Press, New York

Sanakis Y, Ioannidis N, Sioros G, Petrouleas V (2001) A novel S = 7/2 configuration of the Mn cluster of photosystem II. J Am Chem Soc 123:10766–10767

Sivaraja M, Tso J, Dismukes GC (1989) A calcium-specific site influences the structure and activity of the manganese cluster responsible for photosynthetic water oxidation. Biochemistry 28:9459–9464

Smith PJ, Pace RJ (1996) Evidence for two forms of the $g = 4.1$ signal in the $S_2$ state of photosystem II. Two magnetically isolated manganese dimers. Biochim Biophys Acta 1275:213–220

Smith PJ, Åhrling KA, Pace RJ (1993) Nature of the $S_2$ state electron paramagnetic resonance signals from the oxygen-evolving complex of photosystem II: Q-band and oriented X-band studies. J Chem Soc Faraday Trans 89:2863–2868

Szalai VA, Brudvig GW (1996) Formation and decay of the S3 EPR signal species in acetate-inhibited photosystem II. Biochemistry 35:1946–1953

Tso J, Sivaraja M, Dismukes GC (1991) Calcium limits substrate accessibility or reactivity at the manganese cluster in photosynthetic water oxidation. Biochemistry 30:4734–4739

van Vliet P, Rutherford AW (1996) Properties of the chloride-depleted oxygen-evolving complex of photosystem II studied by electron paramagnetic resonance. Biochemistry 35:1829–1839

Weil JA, Bolton JR, Wertz JE (1994) Electron paramagnetic resonance: elementary theory and practical applications. John Wiley & Sons, Inc., New York

Yachandra VK, Guiles RD, Sauer K, Klein MP (1986) The state of manganese in the photosynthetic apparatus. 5. The chloride effect in photosynthetic oxygen evolution. Biochim Biophys Acta 850:333–342

Yamauchi T, Mino H, Matsukawa T, Kawamori A, Ono T-A (1997) Parallel polarization electron paramagnetic resonance studies of the $S_1$-state manganese cluster in the photosynthetic oxygen-evolving system. Biochemistry 36:7520–7526

Zhang C, Styring S (2003) Formation of split electron paramagnetic resonance signals in photosystem II suggests that $\text{Tyrosine}_Z$ can be photooxidized at 5 K in the $S_0$ and $S_1$ states of the oxygen-evolving complex. Biochemistry 42:8066–8076

Zhang C, Boussac A, Rutherford AW (2004) Low-temperature electron transfer in photosystem II: a tyrosyl radical and semiquinone charge pair. Biochemistry 43:13787–13795

Zheng M, Dismukes GC (1996) Orbital configuration of the valence electrons, ligand field symmetry, and manganese oxidation states of the photosynthetic water oxidizing complex: analysis of the $S_2$ state multiline EPR signals. Inorg Chem 35:3307–3319

Zimmermann J-L, Rutherford AW (1984) EPR studies of the oxygen-evolving enzyme of Photosystem II. Biochim Biophys Acta 767:160–167

Zimmermann J-L, Rutherford AW (1986) Electron paramagnetic resonance properties of the $S_2$ state of the oxygen-evolving complex of photosystem II. Biochemistry 25:4609–4615

Zouni A, Witt H-T, Kern J, Fromme P, Krauss N, Saenger W, Orth P (2001) Crystal structure of photosystem II from *Synechococcus elongatus* at 3.8 Å resolution. Nature 409:739–743